

Thermal bath in de Sitter space from holographyChong-Sun Chu^{1,2,*} and Dimitrios Giataganas^{1,†}¹*Physics Division, National Center for Theoretical Sciences, National Tsing-Hua University, Hsinchu 30013, Taiwan*²*Department of Physics, National Tsing-Hua University, Hsinchu 30013, Taiwan*

(Received 4 November 2016; published 31 July 2017)

We consider the AdS/dS CFT correspondence and use holography to study the thermal nature of field theory in de Sitter space. Unlike the temperature of a thermal field theory in flat spacetime, the temperature of a superconformal field theory on de Sitter space is an integral part of the theory and leaves intact the conformal symmetry and supersymmetry. In the dual AdS side with the de Sitter factor written in planar coordinates, there is neither a black hole nor a cosmological horizon like that in static coordinates. Instead we have cosmological expansion of the de Sitter space. We consider a number of different observables, such as the entanglement entropy and Wilson loops corresponding to static and spinning mesons in the field theory, and study their thermal properties using holography. We show clearly how the field theory observables get their thermal properties from the bulk despite the absence of a black hole or cosmological horizon, with the role of the horizon played by the cosmological expansion of the de Sitter factor of the AdS metric.

DOI: [10.1103/PhysRevD.96.026023](https://doi.org/10.1103/PhysRevD.96.026023)**I. INTRODUCTION**

De Sitter spacetime is an important background in cosmology because it not only describes the late time cosmology, but it is also crucial to the description of the inflationary early Universe. In a certain approximation, one may decouple quantum gravity and consider the quantum dynamics of other fields on a background de Sitter spacetime. Using perturbative quantum field theory on de Sitter space [1], one could connect the cosmological perturbation of the Cosmic microwave background (CMB) in terms of the quantum fluctuation of the field theory in a slow roll potential. Among other things, the prediction of a scale invariant spectrum is in excellent agreement with the observational results of CMB and marked a remarkable success for the inflationary scenario. Nevertheless the picture suffers from the η problem for the inflaton mass. A minimally coupled massless scalar field also suffers from large secular infrared effects and it would be nice to have better non-perturbative techniques to deal with them, beyond the often practiced approximation methods such as the dynamical renormalization group (dRG) [2] or stochastic analysis [3].

Recently, by employing a specific dS-slicing coordination of the AdS space

$$ds^2 = dz^2 + \sinh^2(Hz) \frac{-dx_0^2 + dx_i^2}{H^2 x_0^2}, \quad z \geq 0, \quad (1)$$

a duality between type IIB string theory on $\text{AdS}_5 \times S^5$ with dS_4 boundary and the $\mathcal{N} = 4$ maximal superconformal Yang-Mills (SCYM) theory has been proposed [4]. It should

be mentioned that while it is not possible to construct a global supersymmetric field theory on four-dimensional de Sitter spacetime [5,6], the employment of global superconformal symmetry makes it possible. The Lagrangian of the SCYM theory has been constructed in [7]. See also [8–15] for related works. The SCYM theory is a cousin of the $\mathcal{N} = 4$ supersymmetric Yang-Mills theory on flat space and, based on the holographic duality, it has been argued that SCYM theory would also share certain remarkable properties like its cousin, such as exact conformality; $SL(2, Z)$ strong-weak duality; and integrability in some of its sectors. This makes the studies of the quantum $\mathcal{N} = 4$ SCYM field theory a well-motivated problem (e.g., [16]) and it will be the subject of a different paper.

De Sitter field theory has a finite temperature $T = H/(2\pi)$. The temperature of de Sitter space can be most easily seen in the static coordinates of de Sitter space where there is a timelike Killing vector and a (cosmological) horizon exists [17]. However the temperature of de Sitter space Bunch-Davies vacuum is in fact coordinate independent and can be established using the Unruh effect; see, for example, [18]. The temperature of de Sitter space has properties quite different from that of a thermal field theory in flat spacetime: 1. While ordinary temperatures break Poincaré supersymmetry, the de Sitter temperature does not break de Sitter superconformal symmetry. This is partially because the de Sitter temperature is not an independent parameter but is fixed directly in terms of the de Sitter space. 2. In terms of holography, the thermal vacuum of a quantum field theory in flat spacetime is dual to a black hole deep in the bulk. The presence of a black hole, in particular its horizon, changes the behavior of bulk supergravity solutions compared to the case without, and this is how the bulk gravitational dynamics could account

*cschu@phys.nthu.edu.tw

†dgiataganas@phys.cts.nthu.edu.tw

for the properties of the thermal field theory. In [19], a slicing of the AdS bulk space using a de Sitter metric in static coordinates was employed and the authors were able to establish the thermality of the de Sitter field theory by relating it to the cosmological horizon of the de Sitter space, similar to the way the horizon of an AdS black hole does in a typical thermal field theory in flat space.

We are interested in the AdS/dS duality with the de Sitter factor of the AdS metric written in planar coordinates [see (1)] since in order to properly formulate the de Sitter quantum field theory, it is necessary to employ planar coordinates (or the Friedmann-Robertson-Walker (FRW) coordinates, which are related by a redefinition of the time coordinate) where the space is homogeneous. But then there is no longer any horizon in the dual metric and it may seem puzzling how the de Sitter temperature may arise from holography. The main motivation of our work is to see which effects in the bulk of (1) are responsible for the temperature of the de Sitter field theory.

With the de Sitter space written in planar coordinates, it is natural to suspect that the role of the black hole horizon would be played by the cosmological expansion of the AdS bulk. We will demonstrate that this is correct but the involved mechanism is different. For example, in contrast with the effect of the AdS black hole where the presence of the gravitational attraction of the black hole pulls the string along the radial holographic direction, the cosmological expansion pulls the string in the directions orthogonal to the radial direction. We will show how this effect of the cosmological expansion would lead to an interesting causality constraint on the contribution of the string minimal surface to the quark-antiquark potential, which would then lead to an infrared thermal contribution to the potential similar to the one due to the black hole horizon in the more familiar AdS black hole case. This is how the temperature of the de Sitter field theory arises from the bulk (1).

As stated, the presence of de Sitter temperature is compatible with the superconformal symmetry of de Sitter space. As the two- and three-point correlation functions of the theory are completely fixed by the conformal symmetry, this means they depend on the temperature in a trivial way, through the geodesic distance of the space. This is indeed what we found in [4] using the bulk-to-boundary formalism. However this is not the case for other more nontrivial observables. For example, if we consider a Wilson loop operator W_C on the de Sitter field theory, the expectation value of the Wilson loop could depend nontrivially on dimensionless combinations such as LT or AT^2 , where $L(A)$ is the length (area) of the loop C . This is a highly nontrivial problem, especially in the strongly coupled regime. The same holds for several other heavy quark observables like the energy of spinning mesons. The analysis of such nontrivial temperature dependence in strongly coupled field theory in de Sitter space is another motivation of this paper. Notice that gauge/gravity duals in de Sitter were also studied in [20–36]

The plan of the paper is as follows. In Sec. II, as a warm-up exercise, we consider the computation of entanglement entropy in the de Sitter theory and reproduce the expected result directly using the dS-sliced coordinate system. It also serves to demonstrate how to handle some of the difficulties associated with the numerical analysis of a minimal surface in dS-sliced coordinates, which are useful for the subsequent analysis for the meson system. In Sec. III, we set up a heavy quark bound state system with constant interquark distance, which is important for the computation of the static potential between the quarks. Since we work in planar coordinates for dS, there is no cosmological horizon like that in static coordinates. Nevertheless, by computing the energy of the bound system we find a similar thermal behavior as in theories in flat spacetime. We find that the string observables realize a temperature in planar coordinates due to the nonzero expansion rate H of the space. We also discuss in what ways the cosmological expansion and the black hole horizon differ in their effects on the bulk dynamics of strings. In Sec. IV, we consider a spinning heavy quark bound state with constant interquark distance. We regularize the energy and the angular momenta using both the Legendre transformed action and the infinite string solutions corresponding to the mass of heavy quarks. We find that there exists a maximum angular momentum beyond which the bound state ceases to exist. This is similar to the behavior of the bound states in finite temperature field theories in flat spacetime. Section V contains our conclusions and discussions.

II. ENTANGLEMENT ENTROPY

In this section, as a warm-up exercise, we compute the entanglement entropy for a rectangular stripe on dS space using holography [37,38]. The main point of this exercise is to reproduce the expected results directly using the dS-sliced coordinate system. It also serves to demonstrate how to handle some of the difficulties associated with the numerical analysis of a minimal surface in dS-sliced coordinates, which will be useful for the subsequent analysis for the meson system in the next section.

Let us consider a general class of bulk metric of the form

$$ds^2 = g_{\eta\eta}(\eta, z)d\eta^2 + \sum_{i=1}^{d-1} g_{ii}(\eta, z)dx_i^2 + g_{\rho\rho}(\eta, z)dz^2, \quad (2)$$

where $i = 1, \dots, d-1$. In this coordinate patch, the boundary of the space is located at $z = z_{\text{bdy}} = \infty$ and is given by a d -dimensional boundary manifold. We consider a rectangular strip Σ on the boundary described by

$$-\frac{L}{2} \leq x_1 \leq \frac{L}{2}, \quad 0 \leq x_j \leq L_1, \quad (j = 2, \dots, d-1), \quad (3)$$

where L is the width of the strip and $L_1 \gg L$ so as to ensure translational invariance along the x_j space directions. To obtain the entanglement entropy, we need to compute the area of the codimension-2 minimal surface γ_Σ whose boundary is given by Σ . For a static parametrization of the surface

$$x_1 = \sigma, \quad x_j = \sigma_j, \quad z = z(\sigma), \quad \eta = \eta(\sigma), \quad (4)$$

the boundary condition at $\sigma = \pm L/2$ is

$$z\left(-\frac{L}{2}\right) = z\left(\frac{L}{2}\right) = z_{\text{bdy}}, \quad (5)$$

where $g_{ii}(\eta, z_{\text{bdy}}) = \infty$. The entanglement entropy of the chosen region (4) is given by

$$4G_N^{(d+1)} S = \text{Area}(\gamma_\Sigma) = L_1^{d-2} \int d\sigma A(\sigma) \sqrt{D}, \quad (6)$$

where

$$A := \sqrt{g_{22}g_{33}\dots g_{dd}}, \quad D := g_{11} + g_{zz}z'^2 + g_{\eta\eta}\eta'^2. \quad (7)$$

The Hamiltonian is a constant of motion, since there is no explicit σ dependence. Setting it equal to $-c$ we obtain the constraint

$$\frac{Ag_{11}}{\sqrt{D}} = c, \quad (8)$$

which gives a first order ordinary differential equation of z and η :

$$g_{zz}z'^2 + g_{\eta\eta}\eta'^2 + g_{11}\frac{c^2 - A^2g_{11}}{c^2} = 0. \quad (9)$$

The other two equations of motion are obtained by the variation of the action (6) and give

$$\begin{aligned} & \sqrt{D}\partial_\alpha A + \frac{A}{2\sqrt{D}}(\partial_\alpha g_{11} + \partial_\alpha g_{zz}z'^2 + \partial_\alpha g_{\eta\eta}\eta'^2) \\ & - \begin{cases} \partial_\sigma\left(\frac{A}{\sqrt{D}}g_{zz}z'\right) = 0, \\ \partial_\sigma\left(\frac{A}{\sqrt{D}}g_{\eta\eta}\eta'\right) = 0, \end{cases} \end{aligned} \quad (10)$$

where $\partial_\alpha = \partial_\eta$ or ∂_z . Eliminating the square root using the constraint (8), we obtain

$$\begin{aligned} & \frac{g_{11}}{2c}\partial_\alpha(A^2) + \frac{c}{2g_{11}}(\partial_\alpha g_{11} + \partial_\alpha g_{zz}z'^2 + \partial_\alpha g_{\eta\eta}\eta'^2) \\ & + \begin{cases} -c\partial_\sigma\left(\frac{g_{zz}}{g_{11}}z'\right) - c\frac{g_{zz}}{g_{11}}z'' = 0, \\ -c\partial_\sigma\left(\frac{g_{\eta\eta}}{g_{11}}\eta'\right) - c\frac{g_{\eta\eta}}{g_{11}}\eta'' = 0. \end{cases} \end{aligned} \quad (11)$$

The desired minimal surface γ_Σ is obtained from solving the differential Eqs. (8) and (11), subjected to the boundary conditions (5).

For the AdS $_{d+1}$ metric

$$\begin{aligned} ds_{\text{AdS}_{d+1}}^2 &= dz^2 + \sinh^2 Hz ds_{\text{dS}_d}^2, \\ ds_{\text{dS}_d}^2 &= \frac{1}{H^2\eta^2}(-d\eta^2 + dx_i^2), \end{aligned} \quad (12)$$

where $R = 1/H$ is the de Sitter radius and has to be equal to the anti-de Sitter radius [4]. The function (7) and the expressions that appear in the equations of motion are

$$A(\sigma) = \left(\frac{\sinh Hz}{H\eta}\right)^{d-2}, \quad \frac{g_{zz}}{g_{11}} = \frac{H^2\eta^2}{\sinh^2 Hz}, \quad \frac{g_{\eta\eta}}{g_{11}} = -1. \quad (13)$$

Then the Hamiltonian constraint (8) and the equations of motion (11) take the relatively compact form

$$z'^2 - \frac{\sinh^2 Hz}{H^2\eta^2}\eta'^2 + \frac{\sinh^2 Hz}{H^2\eta^2}\left(1 - \frac{1}{c^2}\left(\frac{\sinh^2 Hz}{H^2\eta^2}\right)^{d-1}\right) = 0, \quad (14)$$

$$\begin{aligned} & z'' - 2H \coth(Hz)z'^2 + \frac{2}{\eta}z'\eta' + \frac{\sinh(2Hz)}{2H\eta^2}\eta'^2 \\ & - \frac{\sinh(2Hz)}{2H\eta^2}\left(1 + \frac{d-2}{c^2}\left(\frac{\sinh^2 Hz}{H^2\eta^2}\right)^{d-1}\right) = 0, \end{aligned} \quad (15)$$

$$\eta'' + \frac{1}{\eta}\eta'^2 - \frac{1}{\eta}\left(1 + \frac{d-2}{c^2}\left(\frac{\sinh^2 Hz}{H^2\eta^2}\right)^{d-1}\right) = 0. \quad (16)$$

In an arbitrary number of dimensions the equations can be solved numerically. However, for the case of two-dimensional conformal field theory, the factor $A(\sigma)$ in (13) is equal to the unit and the equations of motion can be solved analytically.

Let us first consider the case of a two-dimensional conformal field theory. The equation of motion (16) for η reads

$$\eta'' + \frac{\eta'^2}{\eta} - \frac{1}{\eta} = 0. \quad (17)$$

This has the solution

$$\eta = \pm\sqrt{\sigma^2 + c_1\sigma + c_2}, \quad (18)$$

with $c_{1,2}$ being constants of integration. Notice that the solution of η does not depend on the Hubble constant H . Similarly Eq. (15) gives

$$z'' - 2H \coth(Hz)z'^2 + \frac{2}{\eta}z'\eta' - \sinh(2Hz)\frac{1 - H^2\eta^2}{2H\eta^2} = 0, \quad (19)$$

and by substituting the solution (18), we get a second order differential equation for $z(\sigma)$:

$$z'' - 2H \coth(Hz)z'^2 + z'\frac{2\sigma + c_1}{\sigma^2 + c_1\sigma + c_2} + \sinh(2Hz)\frac{c_1^2 - 4c_2}{8H(\sigma^2 + c_1\sigma + c_2)^2} = 0. \quad (20)$$

The solution for z then can be written in the compact form as

$$\coth Hz = \pm \frac{c_3}{4} \cdot \frac{4 + c_4(c_1^2 - 4c_2)\sigma}{\sqrt{c_2 + c_1\sigma + \sigma^2}}, \quad (21)$$

where c_3 and c_4 are arbitrary integration constants. To specify the integration constants, we note that due to the symmetry of the problem, the geodesic should be left-right symmetric with respect to x_1 . The geodesic has a turning point in the bulk (z_0, η_0) , which by the symmetry of the space must therefore be located at $\sigma = 0$, and the desired functions z and η must be even functions of σ . We obtain immediately that $\eta_0 = \pm\sqrt{c_2}$, $c_1 = 0$, $c_4 = 0$, and

$$\eta = \sqrt{\sigma^2 + \eta_0^2}. \quad (22)$$

In addition, c_3 can be expressed in terms of the turning point coordinates as $\coth^2 Hz_0 = c_3^2/\eta_0^2$. Now the boundary condition (5) at $\sigma = \pm L/2$ gives $c_3^2 = L^2/4 + \eta_0^2$. Therefore, eliminating c_3 , we get the relation $\sinh^2(Hz_0)/\eta_0^2 = 4/L^2$ between the turning point (z_0, η_0) and L . Note that the Hamiltonian constraint (8) is satisfied by the solutions and by applying it at the turning point for the geodesic it fixes the constant c as $c^2 = 4/(H^2L^2)$. The minimized action is

$$4G_N^{(3)}S = \frac{2}{H} \operatorname{arctanh} \frac{2\sigma}{L} \Big|_0^{L/2-\varepsilon} = R \log \left(\frac{L}{\varepsilon} \right), \quad (23)$$

where $R := 1/H$ is the radius of the AdS space and $\varepsilon \approx 0$ is a UV cutoff imposed in the σ direction of the world sheet. To compare with the field theory, we need to express (23) in terms of the UV cutoff of the field theory. This can be achieved by noting that if we introduce the radial coordinate ρ of the bulk defined by

$$dz = R \frac{d\rho}{\rho}, \quad (24)$$

then the desired UV cutoff is given by

$$R \log \frac{1}{\varepsilon} := z \left(\frac{L}{2} - \varepsilon \right) \approx \frac{1}{2H} \log \frac{4\eta_b^2}{L\varepsilon},$$

$$\text{where } \eta_b := \eta \left(\frac{L}{2} \right) = \sqrt{\frac{L^2}{4} + \eta_0^2}. \quad (25)$$

η_b is the time coordinate for the boundary point of the string. As a result,

$$4G_N^{(3)}S = 2R \log \frac{L}{\varepsilon\eta_b}, \quad (26)$$

where η_b should be treated as an independent parameter apart from L , and we obtain [39,40]

$$S = \frac{c}{3} \log \frac{L}{\varepsilon}, \quad c = \frac{3R}{2G_N^{(3)}}. \quad (27)$$

The entropy (27) has a trivial L dependence as fixed by conformal symmetry. We also note that (27) is the same as the result in the flat space. This should be obvious since the dS-sliced metric (12) can be related to the Poincaré-sliced metric

$$ds^2 = H^{-2} \left(\frac{dr^2}{r^2} + r^2(-dt^2 + dx_i^2) \right) \quad (28)$$

with the coordinate transformation

$$r = \frac{\sinh Hz}{\eta}, \quad t = \eta \coth Hz. \quad (29)$$

Under this coordinate transformation, our minimal surface is mapped to the minimal surface in the Poincaré coordinates with boundary at $r = \infty$. This is precisely the same minimal surface used in the computation of the holographic entanglement entropy for the strip in the Poincaré coordinates.

In the above computation of the holographic entanglement entropy, we have computed the length L_g of the bulk geodesic joining the two points $x_1 = \pm L/2$ on the boundary. As an application, this can be used to reconstruct the boundary correlation function for conformal operators. In general, for a scalar field of mass m in the bulk of AdS₃, it has the lowest energy eigenvalue $H\Delta$ and the bulk propagator from x to x' is given by

$$G(x, x') = \int \mathcal{D}\mathcal{P} e^{-H\Delta L(\mathcal{P})}, \quad (30)$$

where \mathcal{P} is a path joining the two points and $L(\mathcal{P})$ is the proper length of the path \mathcal{P} . In the semiclassical limit, the path integral is localized to its saddle points and is given by a sum over the geodesics. In the present case,

$$G(x, x') = e^{-H\Delta L_g}. \quad (31)$$

According to [41,42], (30) is also equal to the CFT correlator for the dual operator \mathcal{O} in the large N limit. Therefore we

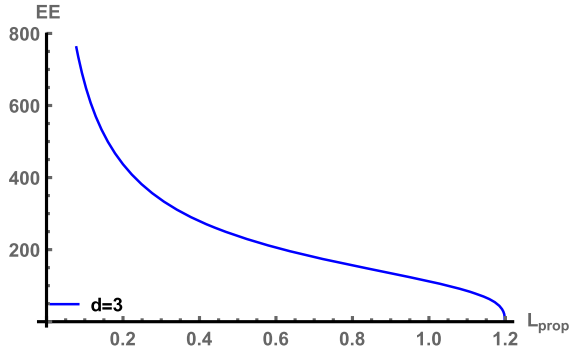


FIG. 1. The absolute value of the entanglement entropy multiplied by $4G_N^{(d)}$ in terms of the proper length for $d = 3$.

obtain in the large N limit and semiclassical approximation the following expression for the two-point function,

$$\langle \mathcal{O}(x)\mathcal{O}(x') \rangle \approx \left(\frac{1}{\epsilon}\right)^{2\Delta} e^{-H\Delta L_g}, \quad (32)$$

where we have regulated the two-point function by adopting a normalization involving an appropriate expression of the cutoff ϵ . Using (26), we obtain

$$\left\langle \mathcal{O}\left(-\frac{L}{2}, t\right) \mathcal{O}\left(\frac{L}{2}, t\right) \right\rangle = \left(\frac{\eta_b}{L}\right)^{2\Delta} \sim \frac{1}{\sigma^{2\Delta}}, \quad (33)$$

where σ is the de Sitter invariant distance. (33) agrees with the result obtained in [4] using the bulk-to-boundary formalism. This is entirely expected since the result is completely determined by conformal invariance.

For higher dimensions, the entanglement entropy for the strip is available in [43]. Here we will consider the numerical solution for the minimal surface in the de Sitter-sliced coordinates. The turning point of the extremal surface in the bulk (z_0, η_0) is located at $\sigma = \sigma_0$. The first order Hamiltonian constraint (14) is satisfied at the turning point trivially, leaving the two initial values independent. Therefore we solve Eqs. (15) and (16) numerically, by specifying the turning point of the surface and extracting from the solutions the proper length

$$L_{\text{prop}} := \frac{L}{\eta_b}, \quad (34)$$

where η_b is the value of η at the boundary. Then we integrate (6) to obtain the entanglement entropy, which we express in terms of the proper length. The computation can be done in arbitrary dimensions. For $d = 2$, it reproduces the analytic result (26), while for higher dimensions $d = 3, 4$ our results for the entanglement entropy are presented in Figs. 1 and 2. The curves are produced by assigning small initial values for η_0 and z_0 and by increasing the value of z_0 to compute the entanglement entropy for different proper lengths. For small proper distance our numerical results hint at the presence of the term

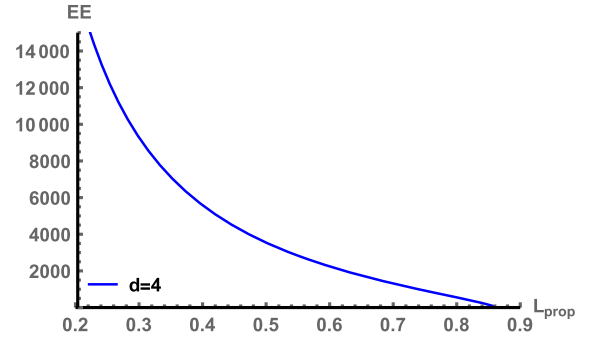


FIG. 2. For the case of $d = 4$.

$$S \propto -\left(\frac{1}{L_{\text{prop}}}\right)^{d-c_1} + \dots, \quad (35)$$

where $c_1 = 2$ offers a reasonable fitting for both plots. This reproduces the expected result of [43].

III. STATIC MESONS IN dS THEORY

To see a nontrivial dependence on the cosmological expansion rate and study its role as temperature, let us introduce heavy massive external quarks and consider expectation values of the Wilson loop operators for space-like loop C in the dS conformal field theory. According to holography [44,45], they are determined in the large N limit, by the minimal surface formed by the string world sheet ending on the loop C on the dS boundary. For convenience let us go to planar coordinates for the dS space by setting $\eta = e^{-2Ht}$, so that we have

$$\begin{aligned} ds_{\text{dS}_{d+1}}^2 &= dz^2 + \sinh^2 Hz ds_{\text{dS}_d}^2, \\ ds_{\text{dS}_d}^2 &= -dt^2 + e^{2Ht} dx_i^2. \end{aligned} \quad (36)$$

One of our motivations in this section is to provide a methodology to study Wilson loops in time dependent strongly coupled theories. This will be done by setting up appropriate boundary conditions on quarks at the boundary of the theory and by using both the Legendre transform formalism and the disconnected string solutions corresponding to the mass of the heavy quarks, in order to regularize the energy and subtract the UV divergences. We note that the analysis of the holographic Schwinger effect in static dS coordinates has been performed in [19]. There a static world sheet corresponding to the Wilson loop has been found and the subtraction of the UV divergences was made by the massive quarks. As already mentioned in the Introduction, a crucial difference with them is that there is no cosmological horizon in our metric. We will elaborate on the similarities and differences among the setups, the string solutions, and the regularization methods in the next sections, where we point out that through our analysis we obtain many interesting insights for the Wilson loop in the expanding spacetime.

A. The string solution

We consider the quark-antiquark pair at the boundary (36) at

$$t = \tau, \quad x_1 = \pm \frac{L}{2} e^{-Ht}, \quad (37)$$

where the \pm sign corresponds to the positions of Q and \bar{Q} , respectively. Note that in contrast to the flat space case, we have specified a specific time dependence for the positions of the quarks, which give them a constant speed

$$v = \pm \frac{HL}{2}, \quad (38)$$

pointing towards each other. This counterbalances the expansion of the dS space and results in a constant dS invariant distance between the quarks

$$\sigma_{\text{inv}}^2(Q, \bar{Q}) = L^2. \quad (39)$$

In other words, we have chosen here to consider a meson of constant size and this is the closest analogy to the flat space case. Motivated by (37), we parametrize the string world sheet as

$$t = \tau, \quad x_1 = e^{-Ht}\sigma, \quad z = z(\sigma). \quad (40)$$

As we will see below, this parametrization guarantees time translation invariance for the Wilson loop and greatly simplifies the problem since the string world sheet is then governed by ordinary differential equations instead of partial differential equations. This is not the case if we have considered the usual static gauge parametrization $t = \tau, x_1 = \sigma, z = z(\sigma)$, which does not satisfy the equations of motion.

It is not difficult to check that the Nambu-Goto (NG) action

$$S = \frac{\sqrt{\lambda}}{4\pi} \int d\sigma d\tau \sqrt{-g} \quad (41)$$

for the parametrization (40) is consistent and gives only one nontrivial equation of motion:

$$\begin{aligned} & (1 - H^2\sigma^2)\sinh^2(Hz(\sigma))z''(\sigma) - H^2\sigma(1 - H^2\sigma^2)z'(\sigma)^3 \\ & - \frac{3H}{2}(1 - H^2\sigma^2)\sinh(2Hz(\sigma))z'(\sigma)^2 \\ & - 2H^2\sigma\sinh^2(Hz(\sigma))z'(\sigma) \\ & - 2H\cosh(Hz(\sigma))\sinh^3(Hz(\sigma)) = 0. \end{aligned} \quad (42)$$

The on-shell action takes the compact form

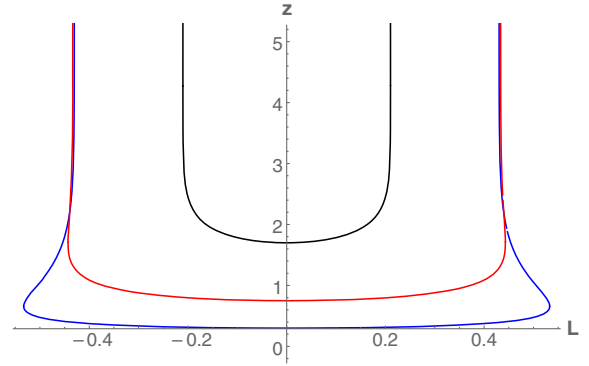


FIG. 3. The string profile for different values of the interquark distance L . The boundary is at the large values of z . We plot string solutions with three different turning points z_0 . The one with smallest L has a string profile that is minimally deformed by the cosmological expansion. The other two string solutions correspond to the same interquark distance L , while the acceptable one has an end point closer to the boundary and is the energetically favorable. The string solution that goes deeper into the bulk is clearly deformed by the cosmological expansion.

$$\frac{4\pi}{T\sqrt{\lambda}}S = \int d\sigma \sinh Hz \sqrt{\sinh^2 Hz + (1 - H^2\sigma^2)z'(\sigma)^2}, \quad (43)$$

where we have integrated the world-sheet time to give a factor of T . Notice that the resulting action is time independent, reflecting the fact that the end points of the string have static invariant distance. For $H\sigma > 1$ the action (43) may become zero or imaginary; this is a common characteristic for the orthogonal Wilson loop action in finite temperature field theories, where H^{-1} here plays the role of the radius of the black hole horizon. Notice that all coordinates in the on-shell action and its equation of motion can be reexpressed in terms of dimensionless quantities using the units of H .

The solution of Eq. (42) can be found numerically and is presented in Fig. 3.¹ For small interquark distances $LH \ll 1$, the profile of the string has the usual U-shape of a hanging chain form with two fixed end points. As the distance between the pair increases, the gravitational effects of the cosmological expansion in the interior of the AdS space give rises to a deformed U-shaped profile with more substantial modification around its turning point.

A couple of remarks are in order:

- (1) A common property of the holographic finite temperature field theories is that to each boundary distance of the string, there are two string solutions extending inside the bulk with different radial dependence [46,47]. This is also the case here. As can be seen in Fig. 3, there are two different string profiles in the bulk with different turning points z_0

¹All plots are in units of $H = 1$ unless otherwise stated.

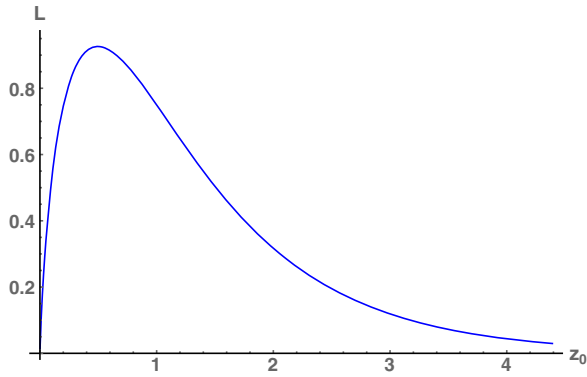


FIG. 4. The interquark distance L in units of H , in terms of the turning point z_0 of the string. For each value of L there exist two string solutions with different turning points and energy. The acceptable one lies on the right branch of the maximum of the curve, since it has lower energy and it is stable. An example of such twin solutions with the same boundary conditions is presented in Fig. 3.

for each boundary separation L . In Fig. 4, we plot L as a function of the turning point z_0 . We find that for an interquark distance less than a certain maximum, namely,

$$L_{\max}H \approx 0.92, \quad (44)$$

there always exists two different connected string solutions. At this point a natural question arises for the reason of the resemblance of our string solutions with the ones in the usual holographic thermal field theories. The mechanism that provides here twin world-sheets solutions is not because of the presence of a black hole in the bulk but is due to the expansion of the dS factor of the AdS space, an effect which is visible when the AdS metric is expressed in the form (1) in terms of the dS-sliced coordinates. Effectively, we have placed the string in the AdS space while keeping fixed the distance of the two boundary string end points by counterbalancing the expansion of the space with a given boundary velocity. However the rest of the string is still affected by the expansion, where the effect is enhanced as one goes deeper in the bulk. At some point the deformation of the connected string becomes so large that the string prefers energetically to break and become two separate strings and this is when the heavy quark bound state dissociates. We note that a similar observation of (44) has been made in [19], where a string solution corresponding to a boundary Wilson loop was obtained in static coordinates. In [19], the pair of quarks is placed symmetrically with respect to the origin by extending the range of r to negative values. Presumably some kind of analytic continuation has been assumed implicitly. The current study on the dynamics of the Wilson loop in planar coordinates reveals many new interesting

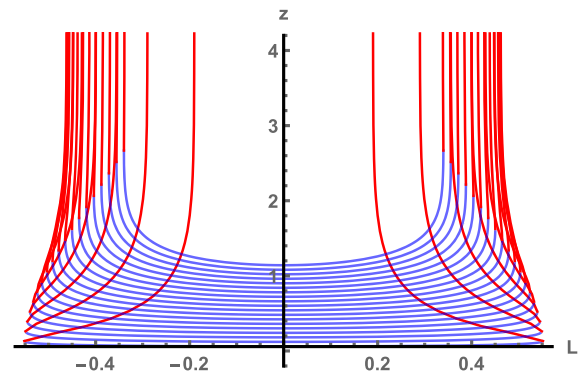


FIG. 5. The string world sheet for different values of the interquark distance L . We observe the changes on the solution as the turning point z_0 moves away from the boundary. In the bottom blue-colored region the derivatives $z'(\sigma)$ are finite, while the red-colored part includes the point of the infinite $z'(\sigma)$ derivative. Notice the string deformation enhancement as it goes closer to the bulk.

properties, especially their thermal properties. The analysis is very interesting on its own and in the following we elaborate on these properties in detail.

- (2) The deformation of the string in the bulk due to the cosmological expansion leads to a minor complication in the numerics.² To obtain the string profile we solve Eq. (42) by selecting the initial value of the holographic distance of the turning point of the world sheet in the bulk z_0 and we shoot from this point towards the boundary. The selection of z_0 specifies the interquark distance L at the boundary. For $\sigma = \sigma_1$ the string has a second turning point at $z_1 = z(\sigma_1)$, where $z'(\sigma_1) = \infty$ (Fig. 3). At this point we need to invert the differential Eq. (42) to obtain the equation for $\sigma(z)$ and to shoot from the point σ_1 with initial conditions $\sigma(z_1) = \sigma_1$ and $\sigma'(z_1) = 0$. The two solutions can be combined to get the full profile of the string. Notice that we need the full solutions in order to find the energy of the string, where we integrate the energy density from $\sigma = \sigma_0$ to $\sigma = \sigma_1$ as a function of σ , and from z_1 to the boundary as a function of z . A series of such solutions are shown in Fig. 5.
- (3) Notice that the deformation on the world sheet due to the cosmological expansion is symmetric in the two edges. This is because we place the Q and \bar{Q} at equal distances from the origin $x_1 = 0$. Nonsymmetric displacement of the pair along the x_1 -axis leads to asymmetric deformation of the string world sheet, enhanced on the side that is further away from the origin. A representative solution is shown in Fig. 6.

²Similar complications have been observed in strings with rotating end points [48]. To simplify the numeric procedure, one may choose a different gauge in the string parametrization. Another such observation has been made in Rindler space [49].

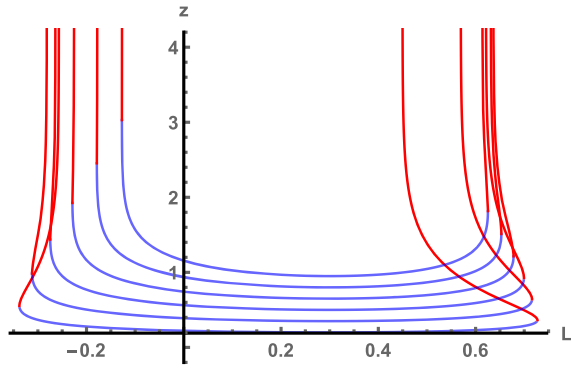


FIG. 6. The heavy quark pair is located asymmetrically with respect to the origin. This asymmetry generates an asymmetric deformation of the bulk string, enhanced on the side that is further away from the origin, in this case at the right side. The midpoint of the string is at $\sigma_0 H = 0.3$.

B. The energy of the bound state

To obtain the energy of the bound state, one needs to regulate the on-shell Nambu-Goto action which is infinite due to the infinite length of the string world sheet. Two subtraction schemes, the Legendre subtraction scheme and the mass subtraction scheme, have been widely used.

As the NG action is a functional of coordinates and the holographic direction of the string world sheet satisfies a Neumann boundary condition, one needs to perform a Legendre transformation to change the boundary condition for the modified action. We point out that the Legendre transform is not diffeomorphic invariant, and for a successful canceling of the UV divergences, we should use the coordinate system ρ (24), which is analogous to the AdS Poincaré coordinates. The Legendre transform of the action in the ρ coordinates is [50,51]

$$S_{\text{Legendre}} = \int d\tau \rho p_\rho \Big|_{\sigma \rightarrow \sigma_1}^{\sigma \rightarrow \sigma_2}, \quad (45)$$

where ρ is the holographic direction, p_ρ is the conjugate momentum

$$p_\rho = \frac{\delta S}{\delta(\partial_\sigma \rho)}, \quad (46)$$

and σ_1 and σ_2 are the end points of the string. Using Eq. (24), we obtain $H\rho p_\rho = p_z$, where

$$p_z = \frac{\delta S}{\delta(\partial_\sigma z)} \quad (47)$$

is the conjugate momentum in the z coordinate, and the desired Legendre term takes the form

$$\tilde{S} = S - \frac{1}{H} \int d\tau p_z \Big|_{\sigma \rightarrow \sigma_1}^{\sigma \rightarrow \sigma_2}. \quad (48)$$

The idea of the mass subtraction scheme is intuitive. For the standard case of $\mathcal{N} = 4$ SYM, a single heavy quark is the end point of a straight string that initiates from the boundary of the space ($z = \infty$) and goes into the bulk. The infinite mass of the quark is given by

$$M_Q = \int_0^\infty dz. \quad (49)$$

The subtraction of this mass from the energy is equivalent to the subtraction using the Legendre term. For the finite temperature $\mathcal{N} = 4$ SYM theory, the gravity dual has a black hole, which introduces a lower bound on the holographic coordinate with a range $[z_h, \infty)$, where z_h is the position of the black hole. Then the corresponding mass for the heavy quark is given by

$$M_Q = \int_{z_h}^\infty dz. \quad (50)$$

Note that apart from allowing us to cancel the UV divergence of the NG action of the connected string world sheet, M_Q now also makes an IR contribution z_h , which is interpreted as a thermal contribution to the bound state energy. On the other hand in the Legendre term (48), information about the thermal properties of the horizon is present through the conjugate momentum and the string solution itself, although in a less direct manner. When computed at the boundary, the black hole contribution is negligible and the Legendre boundary term is equal to that of the zero temperature theory. In general, while both schemes offer the cancellation of the UV divergences, they could differ in their finite IR contribution and the two schemes are not equivalent. The choice of regularization scheme depends on the problem and the physical quantity one desires to compute.

In the present case, due to its intuitive picture, one may want to use the mass subtraction scheme by subtracting out the energy of two single noninteracting quarks moving with the velocity (38). To do this, one needs an appropriate string solution with a single moving end point at the dS boundary,

$$x_0 = \tau, \quad x_1 = \frac{L}{2} e^{-Ht}, \quad (51)$$

with constant velocity. This is however not straightforward to find. In fact the most straightforward string world-sheet parametrization,

$$x_0 = \tau, \quad x_1 = \frac{L}{2} e^{-Ht}, \quad z = z(\sigma), \quad (52)$$

is not a solution of the full system of equations of motion, and a more involved string profile is required. We need to

abandon the straightness of the string in the bulk. We do it by using the same parametrization for the disconnected string with the connected one, where we find that the disconnected string

$$x_0 = \tau, \quad x_1 = \sigma e^{-Ht}, \quad z = \frac{1}{H} \operatorname{arccoth}\left(\frac{2\sigma}{L}\right), \quad (53)$$

satisfies all the equations of motion. Its action reads

$$\frac{4\pi}{T\sqrt{\lambda}} S_Q = \frac{L^2}{4H} \sqrt{1 - \frac{H^2 L^2}{4}} \int_{L/2}^{\sigma_*} d\sigma \left(\sigma^2 - \frac{L^2}{4}\right)^{-3/2}, \quad (54)$$

where σ_* is to be determined. To have real action we require $L/2 < 1/H$ and $\sigma > L/2$ or both the inequalities inverted. Our connected string world sheet satisfies the first one since Eq. (44) holds. The form of the single string solution becomes clear by looking at (53): the string originates from the boundary at $x = L/2$ and bends towards the infinity, the opposite direction to the connected string solution, as it goes into the bulk. However, we have restricted the contribution to the energy (action) to the segment $L/2 \leq \sigma \leq \sigma_*$ since the string is actually moving faster than the speed of light at $\sigma = \sigma_*$ and beyond:

$$v = H\sigma \leq 1 \Rightarrow \sigma \leq \sigma_* := \frac{1}{H}. \quad (55)$$

Beyond this point the string is not causally connected to the part of it that touches the horizon and so should not contribute to the energy. A disconnected string at $x = L/2$ on the boundary can probe the bulk up to distances

$$z_* = \frac{1}{H} \operatorname{arccoth}\left(\frac{2}{HL}\right) \quad (56)$$

and this acts as an infrared cutoff, similar to the role of the black hole horizon in the standard AdS black hole scenario. This is depicted in Fig. 7.

Using (54) we obtain the energy of the single quark

$$\frac{4\pi}{T\sqrt{\lambda}} S_Q = \sqrt{1 - \frac{H^2 L^2}{4}} \frac{\cosh Hz}{H} \Big|_{z \rightarrow \infty} - \frac{1}{H}. \quad (57)$$

The energy of the static quark (57) can be interpreted as the thermal mass of the quark which turns out to depend on the expansion rate of the strongly coupled Universe. By increasing the expansion rate H , the string can access larger distances in the bulk of the space and its energy increases. It is interesting how such a natural expectation arises from the algebra leading to (57). Therefore, the regularized energy for our meson system is given by

$$E_{\text{tot}}(L) = S_{Q\bar{Q}} - 2S_Q, \quad (58)$$

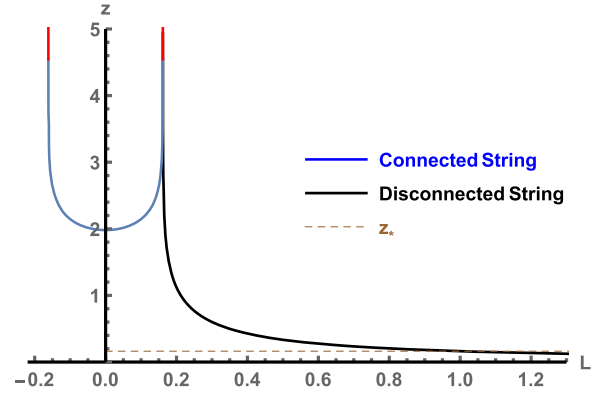


FIG. 7. The connected and the disconnected string solutions. In the disconnected string there is a natural cutoff z_* given by (56) (in this plot at $\sigma_* = 1$) where the cutoff portion of the string is not causally connected to the boundary.

where $S_{Q\bar{Q}}$ is given by the on-shell action (43) and we have subtracted twice the thermal masses of the quarks in the system.

On the other hand, the Legendre subtraction can be performed also without any problem. Similarly the regularized energy is given by

$$E_{\text{tot}}(L) = S_{Q\bar{Q}} - 2S_{\text{UV}}, \quad (59)$$

where S_{UV} is given by

$$\frac{4\pi}{T\sqrt{\lambda}} S_{\text{UV}} = \sqrt{1 - \frac{H^2 L^2}{4}} \frac{\sinh Hz}{H} \Big|_{z \rightarrow \infty}, \quad (60)$$

where we have used the fact that our solution is independent of τ to integrate through the time to get an overall factor of T . The factor of 2 accounts for the contribution from both end points. We have also used the fact that near the end points $\sigma = \pm L/2$, $z \rightarrow \infty$, the differential Eq. (42) is solved by

$$z' = \mp \frac{1}{2HL} e^{2Hz}, \quad (61)$$

where the sign \mp is for $\sigma = \pm L/2$. As a result, near the boundary, p_z is given by

$$p_z = \pm \sqrt{1 - \frac{H^2 L^2}{4}} \sinh Hz, \quad (62)$$

where the sign \pm is for $\sigma = \pm L/2$. We remark that unlike the AdS case in the Poincaré coordinates where the UV divergences of the Wilson loop do not depend on the spatial position of the string, in the present dS-sliced description of the AdS space where the metric becomes time dependent, the UV boundary term is multiplied by a factor that depends on

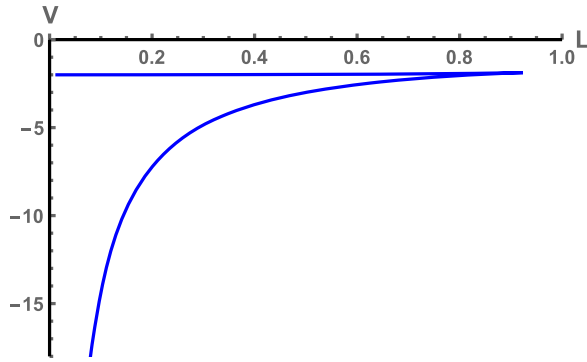


FIG. 8. The regularized energy of the bound state using the Legendre subtraction scheme in terms of the size of the bound state L . We notice that there is a maximum value of distance L with a maximal energy, beyond which there is no minimal surface satisfying the boundary conditions (37). The turning point occurs for negative values of energy, and the almost flat branch corresponds to the nonstable solutions that are energetically unfavorable. Both quantities V and L are dimensionless, normalized with units of H .

the spatial position of the string. This is essential to cancel out the infinity.

By comparing the two regularization schemes in the energy of the bound state, we confirm that they are equivalent in the UV region, since the infinite terms in the actions (57) and (60) have the same asymptotics. In addition, we find that the mass subtraction scheme contributes an additional IR finite term which can be interpreted as the thermal correction to the mass of the quark, leading to a quicker dissociation for larger expansion rates in the strongly coupled space.

Our result for $E_{\text{tot}}(L)$ using the Legendre subtraction scheme is plotted in Fig. 8, while the one using the mass subtraction scheme is plotted in Fig. 9. The regularized energy of the bound state in the AdS/dS space has similarities with that of the bound state in the AdS black hole and the dual finite temperature $\mathcal{N} = 4$ SYM field theory. The energy $E(L)$ has a turning point, indicating a maximum size of the heavy quark bound state with maximal energy for the state, beyond which it does not exist. Moreover, there exist two string solutions that correspond to the same size meson but have different energy. The acceptable solution is the one with the minimum energy which corresponds to the stable and energy preferred state. This resembles the known holographic results of finite temperature field theories including a black hole horizon. Notice that the energy of our solution using the Legendre subtraction scheme does not cross the horizontal axis, in contrast with the use of the mass subtraction scheme. The crossing indicates that the disconnected string has less energy and therefore the crossing point is where the bound state melts to two individual quarks. This is similar to the behavior in thermal field theory with a black hole dual [46,47]. There the mass subtraction scheme was adopted, and it was found that the energy becomes positive at a certain interquark separation $L_* < L_{\text{max}}$. This signifies a

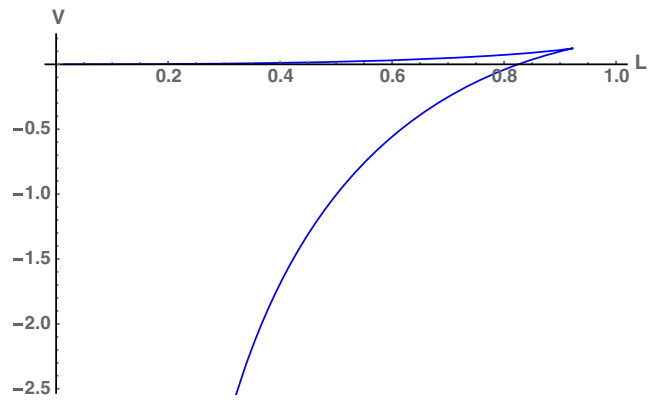


FIG. 9. The regularized energy of the bound state using the mass subtraction scheme in terms of the size of the bound state L . The energy has similar characteristics with the ones in Fig. 8, with the additional ingredient that can take positive values. The crossing point with the horizontal axis is where melting of the bound state to the individual quarks happens. Both quantities V and L are dimensionless using units of H as in Fig. 8.

phase transition where having a pair of straight line strings ending directly on the horizon of the black hole has become the energetically more favorable string configuration.

To summarize, we find that our mesons admit a pair of string solutions for each admissible boundary condition which leads to a bound state similar to the situation of mesons in the usual thermal field theory whose temperature has a holographic origin in terms of a black hole. However the responsible mechanism here is different: it is due to the presence of cosmological expansion in longitudinal directions parallel to the boundary, rather than attraction due to the black hole in the radial/transverse direction [46,47]. By using the mass of the infinite quarks to regularize the energy we find that there is an IR cutoff in the string that is introduced by the need to include only the contribution of that part of the string that is causally connected to the boundary of the space. It resembles the presence of the black hole in the string dynamics. The effects depend on the expansion rate of the spacetime. This signals a very interesting interplay between heavy bound states placed in a dual black hole background and in an expanding strongly coupled Universe. To elaborate further on the properties of a bound state, let us add one more degree of freedom to our system in the next section.

IV. SPINNING MESONS IN dS THEORY

In this section we examine the spinning mesons modeled by rotating hanging strings from the dS boundary.

A. The holographic setup

The spinning string we consider has its two end points on the boundary, corresponding to the quarks of the spinning meson. To consider rotation, it is convenient to rewrite the

planar coordinates metric (36) in the following spherical form:

$$ds^2 = dz^2 + \sinh^2 Hz (-dt^2 + e^{2Ht}(d\rho^2 + \rho^2 d\theta^2 + \rho^2 \sin^2 \theta d\phi^2)). \quad (63)$$

Without loss of generality, we consider rotation along the equator of the sphere with the following parametrization ($0 \leq \sigma \leq L/2$),

$$\begin{aligned} t = \tau, \quad \theta = \frac{\pi}{2}, \quad \phi(\sigma, t) = c + \omega t - \omega f(\sigma), \\ \rho(\sigma, t) = \sigma e^{-Ht}, \quad z = z(\sigma), \end{aligned} \quad (64)$$

where c is a constant to be determined by the two points of the boundary. The function $f(\sigma)$ parametrizes the string world sheet in the bulk and moreover specifies the initial angle for the angular momentum. The boundary conditions of the string are

$$\begin{aligned} z\left(\pm \frac{L}{2}\right) = \infty, \quad \rho\left(\pm \frac{L}{2}, t\right) = \frac{L}{2} e^{-Ht}, \\ \phi\left(\pm \frac{L}{2}, t\right) = \phi_{\pm} + \omega t, \end{aligned} \quad (65)$$

where the two end points of the string are antipodal in the equator, at $\phi_+ = 0$ and at $\phi_- = \pi$. The parametrization (64), (65) describes a string on the equator of the spatial sphere, with antipodal end points having an angular velocity ω , and a component of velocity transverse to the spinning motion and along the axis that connects the

end points, pointing inwards with measure (38), just enough to counterbalance the time dependent expansion of the dS boundary. Below we will solve for the string solution for the region $0 \leq \sigma \leq L/2$ subject to the boundary condition (65) at the end point $\sigma = L/2$. In addition we will require our solution to satisfy

$$z'(\sigma_0) = 0, \quad z(\sigma_0) = z_0, \quad (66)$$

so that we can extend the solution to the other half, $-L/2 \leq \sigma \leq 0$. The constant z_0 is a free parameter that specifies the coordinates of the turning point of the string.

It turns out that the parametrization (64) is a consistent solution to the full system of equations of motion obtained by the NG action only if the function $f(\sigma)$ is given by

$$f(\sigma) = \frac{\log(1 - H^2 \sigma^2)}{2H}. \quad (67)$$

Notice that the function (67) happens to be also part of the coordinate transformation from planar to static coordinates. Physically, it gives a nontrivial σ dependence along the $U(1)$ angle which describes a drag of the string profile in the bulk. We also remark that with a coordinate transformation from planar coordinates to static ones, one can bring the rotating string solution (64) to a form close to a boosted string in static coordinates where the same function (67) also appears.

Having specified the function $f(\sigma)$, we now need to solve the equations of motion to determine $z(\sigma)$ and obtain the string profile in the bulk. The on-shell action is time independent,

$$\frac{4\pi}{\sqrt{\lambda} T} S = \int d\sigma \sqrt{\frac{1 - \sigma^2(H^2 + \omega^2)}{1 - H^2 \sigma^2}} \sinh^2 Hz (\sinh^2 Hz + (1 - H^2 \sigma^2) z'^2) := \int d\sigma \sqrt{D}, \quad (68)$$

and depends explicitly on the world-sheet parameter σ . Variation of the full action gives only one independent equation of motion and reads

$$\begin{aligned} z'' \sinh^2 Hz (1 - H^2 \sigma^2) (1 - (H^2 + \omega^2) \sigma^2) \\ - z'^3 (H^2 + \omega^2) (1 - H^2 \sigma^2)^2 \sigma \\ - \frac{3}{2} z'^2 \sinh 2Hz (1 - H^2 \sigma^2) (1 - (H^2 + \omega^2) \sigma^2) \\ - z' \sinh^2 Hz (\omega^2 + 2H^2 (1 - \sigma^2 (H^2 + \omega^2))) \sigma \\ - \sinh^2 Hz \sinh 2Hz (1 - (H^2 + \omega^2) \sigma^2) = 0. \end{aligned} \quad (69)$$

The string carries energy and angular momentum defined by differentiating the Lagrangian with respect to \dot{t} and $\dot{\phi}$ and integrating the densities along the length of the string:

$$E_{Q\bar{Q}} = 2 \int_0^{L/2} d\sigma \frac{(1 - H^2 \sigma^2) \sqrt{D}}{1 - \sigma^2 (H^2 + \omega^2)}, \quad (70)$$

$$J_{Q\bar{Q}} = 2 \int_0^{L/2} d\sigma \frac{-\omega \sigma^2}{1 - \sigma^2 (H^2 + \omega^2)} \sqrt{D}. \quad (71)$$

The dependence on the parameter ω is continuous and by switching it off $\omega = 0$, the energy (70) is equal to the static on-shell action corresponding to the energy of the bound state of the quark (43), and the angular momentum becomes null. Due to the infinite length of the string, both energy and angular momentum are infinite and a regularization is required. Let us first apply the Legendre subtraction here and comment on the mass subtraction regularization scheme later. The infinite terms that regularize the energy and the angular momentum are given by (48) and applying it to our case we obtain

$$E = E_{Q\bar{Q}} - 2 \sinh Hz \frac{1 - H^2 \frac{L^2}{4}}{\sqrt{1 - \frac{L^2}{4} (H^2 + \omega^2)}} \Big|_{z \rightarrow \infty}, \quad (72)$$

$$J = J_{Q\bar{Q}} - \frac{-L^2 \omega \sinh Hz}{2\sqrt{1 - \frac{L^2}{4} (H^2 + \omega^2)}} \Big|_{z \rightarrow \infty}. \quad (73)$$

For no rotation, the energy (72) is equal to the one in the on-shell action corresponding to the energy of the bound state of the quark (59).

B. The spinning string solutions

The string profile is obtained first by solving the single Eq. (69) on the region $0 \leq \sigma \leq L/2$ and then extending to the other half. That this is possible is based on the following observations: In the region close to the center of the sphere, the string parametrized by (64), (65) does not have a discontinuity along the ϕ coordinate, since the minimum point of the string does not rotate. This can be checked by looking at the equations of motion and noticing that in the full action the derivatives $\partial_\sigma \phi^2$ are multiplied by the term $\sigma^2 \sinh^2 Hz(\sigma)$. The function $z(\sigma)$ is even, with a minimum point at $\sigma = 0$, so its expansion around $\sigma = 0$ is at least of second order. Therefore in the resulting equations of motion the terms involving derivatives of ϕ are all zero at $\sigma = 0$ and the string solution is smooth there too.

Our obtained string profiles are presented in Figs. 10 and 11. The deformation of the U-shaped string inside the bulk is enhanced by the rotation compared to the static case (Fig. 10). Moreover, rotating strings with fixed turning point interquark distance L correspond to surfaces that go

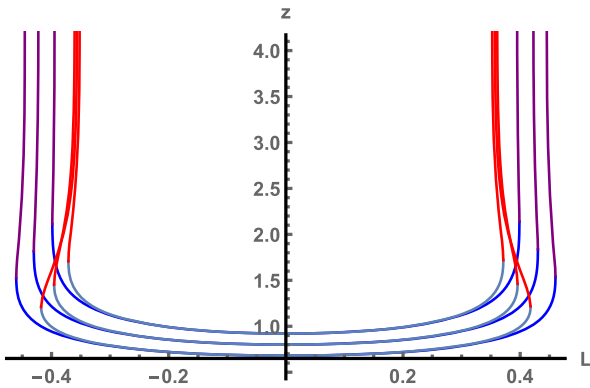


FIG. 10. The string world-sheet solution corresponding to a spinning meson ($\omega = 1$), compared to the static one for fixed bulk distance z_0 . The blue-and-purple-colored outer string solutions are the ones that correspond to the static string, while the inner red-and-cyan-colored strings are the ones corresponding to the spinning state. Notice the spinning strings have less boundary distance between their end points, while the deformation of the U-shaped string is enhanced due to rotation compared to the static configuration.

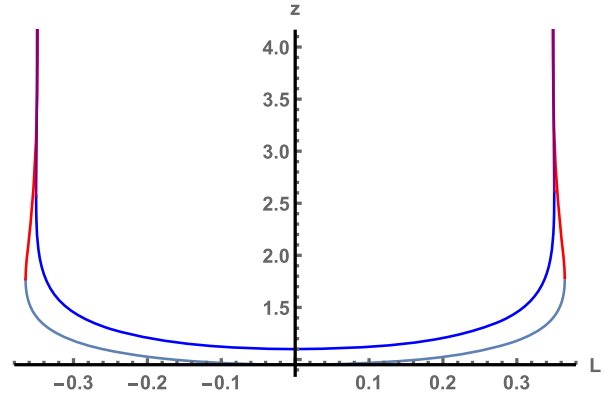


FIG. 11. Spinning and static string world sheets with equal distance string end points. The spinning (red-and-cyan colored) string goes deeper in the bulk and is more deformed compared to the static one. The parameter ω is chosen equal to the unit.

deeper into the bulk compared to the static strings (Fig. 11). This is naturally expected since rotation will tend to increase the distance between the quarks, while the string tension acts in the opposite direction. This is already a hint that rotating strings dissociate easier than static ones; however, for rigorous evidence we need to compute the energy of the bound states.

In the case of the rotating string we have two free parameters that the energy of the state depends on. By fixing the angular velocity of the string and varying the string world-sheet end point we can obtain the function $L(z_0)$. Then we can justify what we have already noticed by comparing the rotating and static strings: the first ones correspond to larger interquark distances for the same turning point z_0 , compared to the latter ones. This is presented in Fig. 12. When we fix the length of the string world sheet and increase the angular velocity, we obtain a function $\omega(z_0)$, where we notice that for the higher angular velocities the minimal surface goes deeper in the bulk in

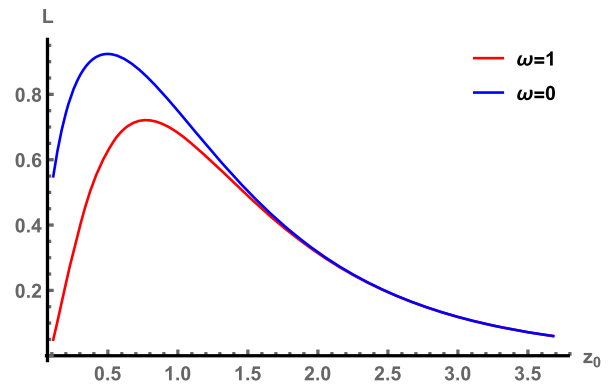


FIG. 12. The function $L(z_0)$ for fixed angular velocity. There are two minimal surfaces for each set of boundary conditions. Increasing angular velocity decreases the maximum length that the state can have.

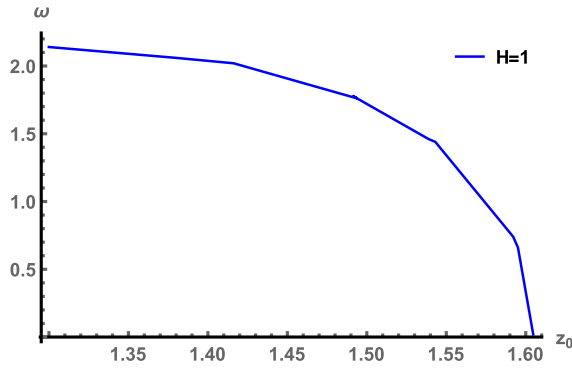


FIG. 13. The function $\omega(z_0)$ for a constant interquark distance at the boundary. A decrease of the angular velocity leads to surfaces that go deeper into the bulk in order to preserve the length on the boundary. This explains naturally the finding of Fig. 12.

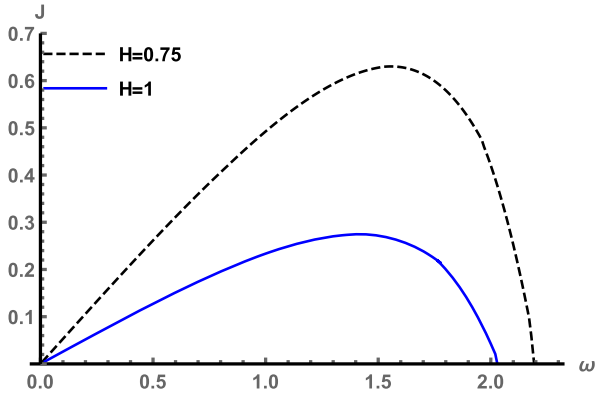


FIG. 14. The angular momentum in terms of the angular velocity. There is a maximum angular momentum that the state can reach for each value of ω_{\max} .

order to preserve the invariant distance at the boundary (Fig. 13). This is in agreement with the previous observations on the string profiles.

To observe the dissociation of the quark bound state in relation with rotation, we fix the length of the state and the cosmological expansion rate H associated with the temperature, and we modify the angular momentum. To keep a state at a constant length as ω increases, we need a world sheet that comes closer to the boundary. We find that the angular momentum of the bound state is increasing for increasing ω until it reaches a maximum value for $\omega = \omega_{\max}$, where the decrease begins. For lower values of H corresponding to lower temperatures, the magnitude of the angular momentum is larger (Fig. 14). This is due to a simple thermal effect on the energy distribution within the quark bound state.

We find that the energy in terms of ω increases for increasing angular velocity until it reaches a maximum value for $\omega = \omega_{\max}$ (Fig. 15). Lower values of H corresponding to lower temperatures lead to higher energies $E(\omega)$ of the bound

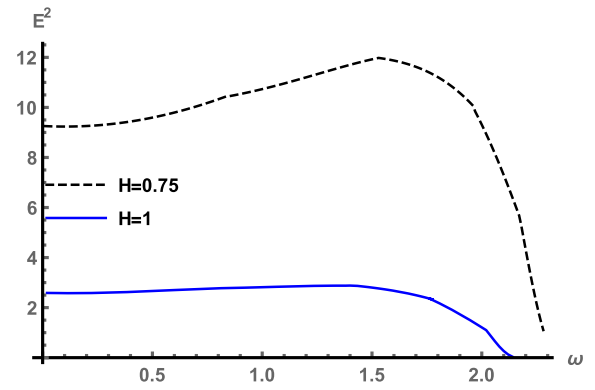


FIG. 15. The square of energy versus the angular velocity $E^2(\omega)$ for a constant interquark distance at the boundary. There is an increase of energy until the angular velocity reaches the value ω_{\max} , and after that it decreases.

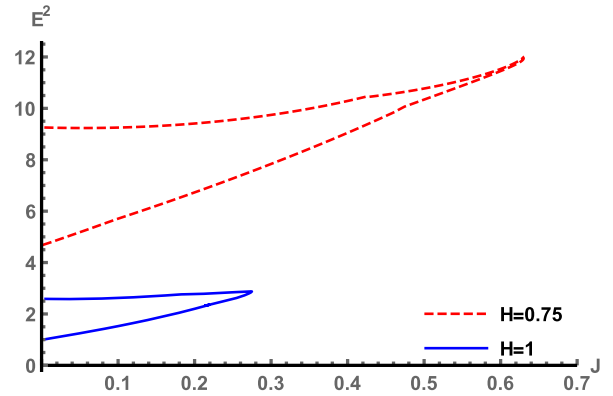


FIG. 16. Energy versus angular momentum for a fixed boundary distance. Notice the maximum reachable angular momentum for the bound state and the fact that for each value of angular momentum the state is allowed to have two energies. The upper segment corresponds to large values of ω . It is unstable and not energetically favorable. The behavior of the bound state is like that of a finite temperature field theory in flat space, with the Hubble constant H corresponding to the temperature of the theory.

state with fixed interquark distance. The maximum of the angular momentum and energy occur for the same value of the angular velocity. Therefore the expression $E^2(J)$ will have a cusp point at $J = J_{\max}$, indicating that a state of fixed interquark distance can reach to a maximum angular momentum. Moreover, for each value of $J < J_{\max}$ the state can be found with both energies, the upper and lower segment in the $E^2(J)$ function (Fig. 16). The upper segment is for large values of ω and large energies and is not energetically preferable. The lower part of the curve depicts the energy of a stable spinning state and has a continuous limit to the spinless state.

The existence of a maximum energy and angular momentum with respect to the angular velocity can be explained by looking at the behavior of the minimal

surface. We have shown that for a fixed interquark distance and increasing angular velocity, the surface has to extend deeper into the bulk in order to preserve the invariant distance at the boundary. There is a critical point at which the effect of the cosmological expansion and the rotation becomes so big that it is no longer possible to have a stable bound state.

To summarize our findings in this section, we conclude that the spinning bound state on a dS CFT theory has all the characteristics of a spinning bound state in a finite temperature dual field theory in flat spacetime. Therefore, it feels the heat bath in a similar way as it would be in the gravity dual theory with a black hole, for example, as in [48]. For a fixed cosmological expansion rate of space, there is a maximal value of the angular momentum which a meson can have. Beyond this value, the meson is interpreted to melt. We note that already in the Legendre subtraction scheme we are able to reproduce the expected thermal effects on the system, like the qualitative dependence of the maximal angular momentum of the meson on the melting temperature. We do not expect that the mass subtraction scheme would produce anything qualitatively different.

V. CONCLUSIONS AND DISCUSSIONS

In this paper we have used holography to examine the thermal properties of the de Sitter field theories in planar coordinates. We have studied heavy quark probes placed in a strongly coupled de Sitter Universe and obtained new interesting insights. A heavy quark and antiquark pair was placed on the dS boundary, where each quark has a constant speed pointing to each other in order to counterbalance the expansion of the spacetime. The heavy meson bound state has a constant invariant interquark distance which corresponds to a time-translational invariant world sheet. We have discussed the physical effects on string configurations due to the presence of cosmological expansion in the bulk. We have compared the Legendre subtraction and the mass subtraction schemes for the regularization of the energy. Using the latter, we find a natural IR cutoff in the dynamics of the disconnected string, imposed by keeping the contribution of the portion of the string that is causally connected to the boundary of the space. The IR cutoff in the strongly expanding Universe depends on the inverse rate of its expansion and resembles the role of the black hole horizon on the dynamics of the disconnected string. We find that an increase of the expansion rate leads to easier dissociation of the heavy quark bound state. Our findings not only fully reproduce the expected thermal properties of the meson bound state system, they also show a very interesting analogy between heavy bound states placed in a dual black hole background and in an expanding strongly

coupled Universe. It would be interesting to independently confirm the thermal behavior noticed in the heavy quark system by computing correlators in the strongly coupled de Sitter theory, where their form would reveal clearly the thermal properties.

By examining the spinning heavy quark bound states, our system gets one more degree of freedom. We observe that there is a maximum angular momentum beyond which the spinning bound state ceases to exist. We compute the energy of the spinning meson in terms of its angular momentum and conclude that the spinning string realizes the Hawking temperature. It would be very interesting to develop a methodology for other observables in the gravity dual of dS field theories, especially the ones whose evaluation in flat thermal field theories depends heavily on the presence of a black hole horizon, like the jet quenching, and to examine how the generic formulas of [52] would be modified in the present setup. Along these lines we mention the interesting study of fluctuation and dissipation in de Sitter space [53].

It is worth noting that the effect of the cosmological expansion of the de Sitter factor persists in the bulk and its effect on the string world sheet is evident. However, the effect is different compared to the strings placed in a black hole background where the tidal gravitational attraction of the black hole tends to pull and deform the string in the radial direction, while the cosmological expansion of the de Sitter factor of the AdS space affects the string in the longitudinal directions parallel to the boundary.

In this paper we have considered de Sitter space written in planar or conformal coordinates. Nevertheless we show that by a suitable choice of ansatz for the string world sheet, one can eliminate from the effective system all the time dependence consistently. By doing that we end up with a time invariant system and ordinary differential equations which are solvable, instead of the more involved partial differential equations. Therefore, the consideration in this paper may also provide some guidance towards the study of other observables in general time dependent theories.

ACKNOWLEDGMENTS

We would like to thank Koji Hashimoto and J. Pedraza for useful discussions. We also thank the participants of the Academic Program ‘‘Holography and Topology of Quantum Matter’’ (APCTP) for discussions and the hospitality of APCTP during the final stage of this work. This work is supported in part by the National Center of Theoretical Science (NCTS) and the Grants No. 101-2112-M-007-021-MY3 and No. 104-2112-M-007-001 -MY3 of the Ministry of Science and Technology of Taiwan.

- [1] N. D. Birrell and P. C. W. Davies, *Quantum Fields in Curved Space* (Cambridge Univ. Press., Cambridge, England, 1982).
- [2] See, for example, C. P. Burgess, L. Leblond, R. Holman, and S. Shandera, Super-Hubble de Sitter fluctuations and the dynamical RG, *J. Cosmol. Astropart. Phys.* **03** (2010) 033; Breakdown of semiclassical methods in de Sitter space, *J. Cosmol. Astropart. Phys.* **10** (2010) 017.
- [3] A. A. Starobinsky and J. Yokoyama, Equilibrium state of a selfinteracting scalar field in the de Sitter background, *Phys. Rev. D* **50**, 6357 (1994).
- [4] C.-S. Chu and D. Giataganas, AdS/dS CFT correspondence, *Phys. Rev. D* **94**, 106013 (2016).
- [5] K. Pilch, P. van Nieuwenhuizen, and M. F. Sohnius, de Sitter superalgebras and supergravity, *Commun. Math. Phys.* **98**, 105 (1985).
- [6] J. Lukierski and A. Nowicki, All possible de Sitter superalgebras and the presence of ghosts, *Phys. Lett.* **151B**, 382 (1985).
- [7] T. Anous, D. Z. Freedman, and A. Maloney, de Sitter supersymmetry revisited, *J. High Energy Phys.* **07** (2014) 119.
- [8] K. Hristov, A. Tomasiello, and A. Zaffaroni, Supersymmetry on three-dimensional Lorentzian curved spaces and black hole holography, *J. High Energy Phys.* **05** (2013) 057.
- [9] D. Cassani, C. Klare, D. Martelli, A. Tomasiello, and A. Zaffaroni, Supersymmetry in Lorentzian curved spaces and holography, *Commun. Math. Phys.* **327**, 577 (2014).
- [10] P. de Medeiros and S. Hollands, Conformal symmetry superalgebras, *Classical Quantum Gravity* **30**, 175016 (2013).
- [11] P. de Medeiros and S. Hollands, Superconformal quantum field theory in curved spacetime, *Classical Quantum Gravity* **30**, 175015 (2013).
- [12] D. Cassani and D. Martelli, Supersymmetry on curved spaces and superconformal anomalies, *J. High Energy Phys.* **10** (2013) 025.
- [13] G. Festuccia and N. Seiberg, Rigid supersymmetric theories in curved superspace, *J. High Energy Phys.* **06** (2011) 114.
- [14] T. T. Dumitrescu, G. Festuccia, and N. Seiberg, Exploring curved superspace, *J. High Energy Phys.* **08** (2012) 141.
- [15] C. Klare and A. Zaffaroni, Extended supersymmetry on curved spaces, *J. High Energy Phys.* **10** (2013) 218.
- [16] C. S. Chu and Y. Koyama, Adiabatic regularization for gauge field and the conformal anomaly, *Phys. Rev. D* **95**, 065025 (2017).
- [17] G. W. Gibbons and S. W. Hawking, Cosmological event horizons, thermodynamics, and particle creation, *Phys. Rev. D* **15**, 2738 (1977).
- [18] M. Spradlin, A. Strominger, and A. Volovich, Les Houches lectures on de Sitter space, [arXiv:hep-th/0110007](https://arxiv.org/abs/hep-th/0110007).
- [19] W. Fischler, P. H. Nguyen, J. F. Pedraza, and W. Tangarife, Holographic Schwinger effect in de Sitter space, *Phys. Rev. D* **91**, 086015 (2015).
- [20] S. Hawking, J. M. Maldacena, and A. Strominger, de Sitter entropy, quantum entanglement and AdS/CFT, *J. High Energy Phys.* **05** (2001) 001.
- [21] A. Buchel, Gauge/gravity correspondence in accelerating universe, *Phys. Rev. D* **65**, 125015 (2002).
- [22] A. Buchel, P. Langfelder, and J. Walcher, On time dependent backgrounds in supergravity and string theory, *Phys. Rev. D* **67**, 024011 (2003).
- [23] O. Aharony, M. Fabinger, G. T. Horowitz, and E. Silverstein, Clean time dependent string backgrounds from bubble baths, *J. High Energy Phys.* **07** (2002) 007.
- [24] V. Balasubramanian and S. F. Ross, The dual of nothing, *Phys. Rev. D* **66**, 086002 (2002).
- [25] M. Alishahiha, A. Karch, E. Silverstein, and D. Tong, The dS/dS correspondence, *AIP Conf. Proc.* **743**, 393 (2004).
- [26] S. F. Ross and G. Titchener, Time-dependent spacetimes in AdS/CFT: Bubble and black hole, *J. High Energy Phys.* **02** (2005) 021.
- [27] V. Balasubramanian, K. Larjo, and J. Simon, Much ado about nothing, *Classical Quantum Gravity* **22**, 4149 (2005).
- [28] T. Hirayama, A holographic dual of CFT with flavor on de Sitter space, *J. High Energy Phys.* **06** (2006) 013.
- [29] J. He and M. Rozali, On bubbles of nothing in AdS/CFT, *J. High Energy Phys.* **09** (2007) 089.
- [30] J. A. Hutasoit, S. P. Kumar, and J. Rafferty, Real time response on dS(3): The topological AdS black hole and the bubble, *J. High Energy Phys.* **04** (2009) 063.
- [31] D. Marolf, M. Rangamani, and M. Van Raamsdonk, Holographic models of de Sitter QFTs, *Classical Quantum Gravity* **28**, 105015 (2011).
- [32] J. Blackman, M. B. McDermott, and M. Van Raamsdonk, Acceleration-induced deconfinement transitions in de Sitter spacetime, *J. High Energy Phys.* **08** (2011) 064.
- [33] M. Li and Y. Pang, Holographic de Sitter universe, *J. High Energy Phys.* **07** (2011) 053.
- [34] L. Anguelova, P. Suranyi, and L. C. R. Wijewardhana, De Sitter space in gauge/gravity duality, *Nucl. Phys.* **B899**, 651 (2015).
- [35] S.-J. Zhang, B. Wang, E. Abdalla, and E. Papantonopoulos, Holographic thermalization in Gauss-Bonnet gravity with de Sitter boundary, *Phys. Rev. D* **91**, 106010 (2015).
- [36] V. Vaganov, Holographic entanglement entropy for massive flavours in dS₄, *J. High Energy Phys.* **03** (2016) 172.
- [37] S. Ryu and T. Takayanagi, Holographic Derivation of Entanglement Entropy from AdS/CFT, *Phys. Rev. Lett.* **96**, 181602 (2006).
- [38] V. E. Hubeny, M. Rangamani, and T. Takayanagi, A covariant holographic entanglement entropy proposal, *J. High Energy Phys.* **07** (2007) 062.
- [39] J. Maldacena and G. L. Pimentel, Entanglement entropy in de Sitter space, *J. High Energy Phys.* **02** (2013) 038.
- [40] W. Fischler, S. Kundu, and J. F. Pedraza, Entanglement and out-of-equilibrium dynamics in holographic models of de Sitter QFTs, *J. High Energy Phys.* **07** (2014) 021.
- [41] V. Balasubramanian and S. F. Ross, Holographic particle detection, *Phys. Rev. D* **61**, 044007 (2000).
- [42] T. Banks, M. R. Douglas, G. T. Horowitz, and E. J. Martinec, AdS dynamics from conformal field theory, [arXiv:hep-th/9808016](https://arxiv.org/abs/hep-th/9808016).
- [43] S. Ryu and T. Takayanagi, Aspects of holographic entanglement entropy, *J. High Energy Phys.* **08** (2006) 045.
- [44] J. M. Maldacena, The large n limit of superconformal field theories and supergravity, *Adv. Theor. Math. Phys.* **2**, 231 (1998).
- [45] E. Witten, Anti-de Sitter space and holography, *Adv. Theor. Math. Phys.* **2**, 253 (1998).

- [46] S.-J. Rey, S. Theisen, and J.-T. Yee, Wilson-Polyakov loop at finite temperature in large N gauge theory and anti-de Sitter supergravity, *Nucl. Phys.* **B527**, 171 (1998).
- [47] A. Brandhuber, N. Itzhaki, J. Sonnenschein, and S. Yankielowicz, Wilson loops in the large N limit at finite temperature, *Phys. Lett. B* **434**, 36 (1998).
- [48] K. Peeters, J. Sonnenschein, and M. Zamaklar, Holographic melting and related properties of mesons in a quark gluon plasma, *Phys. Rev. D* **74**, 106008 (2006).
- [49] E. Caceres, M. Chemicoff, A. Guijosa, and J.F. Pedraza, Quantum fluctuations and the Unruh effect in strongly-coupled conformal field theories, *J. High Energy Phys.* **06** (2010) 078.
- [50] N. Drukker, D. J. Gross, and H. Ooguri, Wilson loops and minimal surfaces, *Phys. Rev. D* **60**, 125006 (1999).
- [51] C.-S. Chu and D. Giataganas, UV-divergences of Wilson loops for gauge/gravity duality, *J. High Energy Phys.* **12** (2008) 103.
- [52] D. Giataganas, Probing strongly coupled anisotropic plasma, *J. High Energy Phys.* **07** (2012) 031.
- [53] W. Fischler, P. H. Nguyen, J. F. Pedraza, and W. Tangarife, Fluctuation and dissipation in de Sitter space, *J. High Energy Phys.* **08** (2014) 028.